Improving a new sparse-coding algorithm dedicated to SAR images with a coeffcient of variation map

Sonia Tabti, Luisa Verdoliva, Giovanni Poggi

Improving a new sparse-coding algorithm dedicated to SAR images with a coeffcient of variation map

Sonia Tabti, Luisa Verdoliva, Giovanni Poggi

***Abstract*—In this paper, we propose a sparsity-based despeckling approach. The first main contribution of this work is the elaboration of a sparse-coding algorithm adapted to the statistics of SAR images. In fact, in most of the sparse-coding algorithms dedicated to SAR data, a logarithmic transform is applied on the data to turn the speckle modeled by a multiplicative noise into an additive noise, then, a Gaussian prior is used. However, using a more suitable prior for SAR data avoids introducing artifacts, as shown in the obtained results. The second main contribution proposed is to evaluate how computing a map predicting the sparsity degree of each patch could bring an improvement compared to a traditional sparse-coding approach with a low-error rate based stopping criterion.**

***Index Terms*—Patches, sparsity, coefficient of variation, denoising, despeckling, SAR images.**

I. Introduction

The aim of this work is to elaborate a despeckling algorithm using a sparsity-based approach dedicated to SAR images. This type of image is sythetized after an electro-magnetic wave is sent on earth surface and backscaterred. Consequently, fluctuations are observed: speckle, which can be modeled according to Goodman's model by a multiplicative noise following a gamma distribution in the case of intensity SAR images. The quality of SAR images can be improved through the multilooking process. Its effect on an image is speckle reduction at the price of resolution degradation by computing for each pixel either the mean of L neighboring pixels in the image of interest or computing a temporal mean it the image is multi-temporal. The number L is referred to as the number of looks.

The principle of a sparsity-based approach is to approximate a small window (of typical size 8×8) extracted from an image, called a patch, by a sparse linear combination of atoms which are the elements of a dictionary $\boldsymbol{D}$ as expressed by the next equation:

$$\min_{\boldsymbol{u}_i} ||\boldsymbol{D}\boldsymbol{u}_i - \boldsymbol{x}_i||_2^2 \quad \text{st} \quad \phi(\boldsymbol{u}_i) \quad \text{is sparse} \tag{1}$$

where $\boldsymbol{x}_i$ is a patch, $\boldsymbol{u}_i$ is the corresponding vector of sparse coefficients, and ϕ is the sparse regularization term.

A standard dictionary-based approach, eg. the K-SVD (Singular Value Decomposition) algorithm [1], is divided in two steps repeated until a stopping criterion is satisfied. The first step is the sparse-coding, ie. the computation of the coefficients of the sparse linear combination which depends on the choice of the prior ϕ. It can be convex with for instance the ℓ_1-norm: $\phi(\boldsymbol{u}) = |\phi|_1$ and the problem can be solved with a Basis-Pursuit algorithm for instance [2]. It can also be non-convex, for example, in the case of an ℓ_0 pseudo-norm, $\phi(\boldsymbol{u}) = ||\boldsymbol{u}||_0$, which counts the number of non-zero elements in $\boldsymbol{u}$, and this number is called: the sparsity degree. One can use greedy approaches in order to approximate the solution of this NP-hard and non-convex problem. The OMP (Orthogonal Matching Pursuit) [3] procedure is often used for this purpose. The second step of a dictionary-based approach is the update of the elements of the dictionary taking the first step into account.

In this work, we suppose that the dictionary is already learned on patches extracted from logarithmically-transformed multi-look SAR images with K-SVD in order to simplify the optimization problems we will have to face. Consequently, we will only have to develop a sparse coding algorithm dedicated to SAR data (see section IV). We will also compute a sparsity-degree map for each patch of the image (see section III-B).

II. Related Works

Many approaches use sparse representations for SAR image despeckling. Most of them apply a logarithmic transform to the image of interest in order to turn multiplicative noise into additive noise. Different data-fidelity terms are then used such as an the Euclidean distance or the Fisher-Tippett distribution which coresponds to log-transformed gamma distribution. Many regularization terms inducing sparsity can also be used such as the ℓ_1 norm, the ℓ_0 pseudo-norm. In [4], the authors propose to use:

$$||\boldsymbol{A}_i||_{1,2} = \sum_{j=1}^{k} ||\boldsymbol{\alpha}^j||_1^2 \tag{2}$$

where each column of the matrix $\boldsymbol{A}_i$ is a vector of sparse coefficients associated to a patch belonging to an i-th cluster of similar patches and $\boldsymbol{\alpha}^j$ is the j-th row of $\boldsymbol{A}_i$. This matrix norm enforces similar patches to have similar estimates.

In [5], the following TV regularization term is proposed:

$$\Lambda(|(\nabla \boldsymbol{x})_p|, f) = \begin{cases} 0 & \text{if } |(\nabla \boldsymbol{x})_p| = 0, f = 0 \\ |(\nabla \boldsymbol{x})_p|^f & \text{otherwise} \end{cases} \tag{3}$$

where p is the pixel index and f is an input parameter such that if $f = 0$ this regularization term coresponds to an ℓ_0

S. Tabti performed this work during her postdoctoral stay at the DIETI and is now a post-doctoral fellow at the GREYC, CNRS-University of Caen, France.

L. Verdoliva and G. Poggi are with the DIETI, Università Federico II di Napoli, Italy.

E-mails: sonia.tabti@unicaen.fr, verdoliv@unina.it, poggi@unina.it.

pseudo-norm, if $f = 1$, it coresponds to an ℓ_1 norm. A convex approximation of this regularization term is also proposed in order to use convex optimization techniques. The authors framework is consequently composed of a few simple steps and the main one boils down to solving a system with a conjugate-gradient method.

Different types of dictionaries can be found in the litterature. There are fixed dictionaries, for instance wavelets or curvelets. The despeckling method proposed in [6] uses curvelets and shows that a prior based on a 2D Generalized Auto-Regressive Conditional Heteroscedastic model (2D-GARCH-GG) is a justified choice for SAR data curvelet coefficients. The results obtained by the authors seem to preserve well edges but no results on Very High Rezolution (VHR) SAR images are shown.

Other dictionaries are learned on the SAR image itself (adaptive dictionaries). In most of standard adaptive approaches, dictionaries are composed of patches and obtained with algorithms dedicated to natural images (eg. : K-SVD, online dictionary learning algorithm [7]). Other adaptive approaches learn dictionaries of PCA (Principal Componenet Analysis) bases, that is to say, after a clustering step of similar patches, a PCA is computed over each cluster and a dictionary coresponds to the eigenvectors matrix associated to the cluster. A further step is added in [8] such that patches are classified in two labels, homogeneous and heterogeneous, using a coefficient of variation so homogeneous and heterogeneous patches are despeckled with two different methods. Table I presents a summary of some approaches in the literature.

III. Preleminary study in the Gaussian case

In this section, a study is presented in order to evaluate within a sparse-coding procedure whether computing a map predicting the optimal sparsity degree of each patch of the image provides better denoising results than selecting the same sparsity degree for all the patches of an image. The type of noise is Gaussian since we do not possess nearly noiseless SAR images and consequently we cannot compute the difference between noiseless and restored data.

A. Computation of the Oracle Sparsity degree Map (OSDM)

This work relies on the hypothesis that different sparsity degrees should be imposed for each patch in the image instead of imposing the same sparsity degree for each patch. For example, a complicated structure as a target or an edge should be represented by more than one atom in its sparse approximation, in opposition with a flat patch, which needs only one atom to represent it. This claim is illustrated by the Oracle Sparsity Degree Map (OSDM) in figure 3 (d). To obtain it we:

- produced 100 noisy realizations of each patch in the image Barbara;
- denoised all these realizations by sparse approximation with different fixed sparsity degrees (from 1 to 4) using:
  - an OMP,
  - a dictionary learned on the noisy patches with the K-SVD algorithm (see fig. 1),
- computed for each patch the sparsity degree which provided the smallest Mean Square Error (MSE).

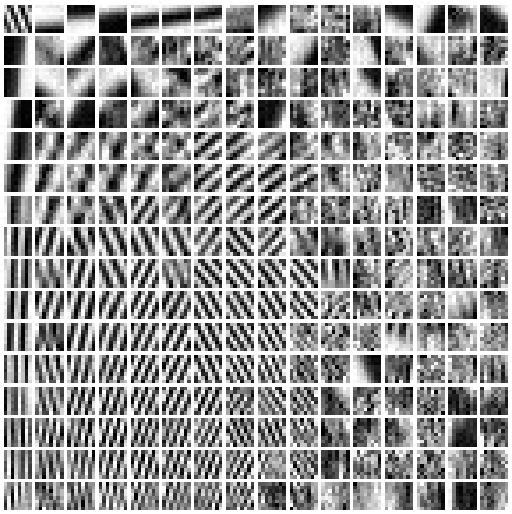

Fig. 1. Dictionary learned with K-SVD on noisy patches of Barbara. It is composed of 256 atoms of size 8×8

To summarize, the OSDM is a map of the optimal sparsity degree for each patch, in the MSE sense, with a given dictionary. In section III-C, it is used as a denoising-guide which will allow us to evaluate how such a map could improve the performance of a simple sparsity-based approach in comparison with the same approach using a fixed sparsity degree for each patch. A strong level of Gaussian noise, $\sigma = 30$, is used in this study in order to obtain conclusions close to the ones we could obtain with SAR images. In fact, they suffer from speckle modeled as strong multiplicative noise. The size of the patches used in this paper is always: 8×8.

B. Computation of the Sparsity Degree Map (SDM) based on the coefficient of variation

In this section, we explain how to compute the Sparsity Degree Map (SDM) based on a Coefficient of Variation Map (CVM) computed on a noisy image. We first recall that the coefficient of variation of a patch $\boldsymbol{x}$ (of size 8×8 in this experiment) is defined by the next formula:

$$\mathcal{C}_v(\boldsymbol{x}) = \frac{\sigma_{\boldsymbol{x}}}{\mu_{\boldsymbol{x}}} \tag{4}$$

where $\sigma_{\boldsymbol{x}}$ is the standard deviation of the patch $\boldsymbol{x}$ and $\mu_{\boldsymbol{x}}$ is the mean of $\boldsymbol{x}$. It is widely used in SAR imagery, for classification purpose for instance, since it measures the heterogeneity of a region: the higher the value of the coefficient, the more heterogeneous is the region. We obtain a CVM by computing the coeffcient of variation of each patch in the image. To ensure the smoothness of the map, it is better to pre-filter the noisy image before computing the CVM. In this study, the pre-filtering is performed by sparse approximation of each patch in the image using an OMP with a fixed sparsity degree, then averaging the patches to

Paper	data-fidelity term	dictionary-type	prior	optimization / details	collaborative-filter
[6]	Gaussian	Curvelets	2D-GARCH-GG	2D-GARCH-GG parameters: ML, Curvelet coefficients: MAP	x
[9]	Nakagami-Rayleigh	K-SVD (off-line, no details)	ℓ_0	S-OMP [10], close to [11]	yes
[4]	Euclidean distance + target preserving term	Online dictionary learning [7]	$\|\|\boldsymbol{A}_i\|\|_{1,2}$	LARS [12]	yes
[13]	Fisher-Tippett	x	improvement of TV	Variable splitting + Augmented Lagrangian as in [14]	x
[8]	Euclidean distance	PCA dictionary for each patch	ℓ_1 + SCN	dictionary update: SAIST [15]	yes (+classification)
[16]	Euclidean distance	PCA dictionary for each patch	ℓ_1 + SCN adapted to SAR data	Same as in [17]	yes
[18]	Euclidean distance	log-K-SVD	ℓ_0	Adapted filtering	x
[5]	Euclidean distance	x	TV or ℓ_1 or ℓ_0	Conjugate Gradient	x
[19]	Euclidean distance	undercomplete K-SVD sub-dictionaries	ℓ_0		yes
[20]	GLR gamma noise	K-medoids	1-sparse		x

TABLE I
SUMMARY OF SOME DESPECKLING PROCEDURES BASED ON SPARSE REPRESENTATIONS.

obtain the whole image. The results of the pre-filtered images with a sparsity degree k equals to 3 and 1 resp. and the corresponding CVM's are presented in figures 3 (e), (i) resp. on the Barbara image.

The whole procedure of the sparsity degree map computation is described in the next steps:

- Computation of the CVM on the pre-filtered image.
- Application of the K-Means algorithm on the CVM using $k_{\max}$ labels (meaning for a sparsity degree ranging from 1 to $k_{\max}$).
- Sorting of the centroids CV values so the highest CV is associated to the biggest sparsity degree and so on.

Since the histogram on figure 2 shows that the most used sparsity degrees to denoise the Barbara image are ranging between 1 and 3 and the proportion of patches represented with more than 4 atoms is very low, we decided to always set $k_{\max} = 4$. We explain how we obtained this histogram in section III-C. This observation stands on other tested images.

One can compare the visual aspect of the OSDM introduced in section III-A and the SDM's with $k = \{1, 3\}$ in figures 3, (d), (f), (j). In spite of the fact that the OSDM and the SDM's are not perfectly similar, we observe that SDM's are accurate, in the sense that they suggest using a sparsity degree equals to one in homogeneous areas and higher sparsity degrees within edges and textures which improves the quality of the denoising as demonstrated in section III-C. Note that the SDM obtained with $k = 1$ is smoother than the the SDM obtained with $k = 3$.

C. Does imposing an optimal sparsity degree to each patch improve denoising results?

In this section, we use the OSDM and the SDM's (with a sparsity degree equals to one and three previously computed) in order to denoise the image of Barbara and compare these results with those obtained with the same fixed sparsity degree for all the patches (equals to one and three resp. also) on the same noise realization. To perform the denoising with a fixed sparsity degree, we proceed the same way as the pre-filtering described in section III-B. To denoise the image using the sparsity maps, we denoise each patch by a sparse approximation using an OMP with the corresponding sparsity degree in the map.

Figure 3 shows the results of this comparison. We observe that the denoising result obtained with the OSDM is the best in term of visual quality and PSNR as expected. We also observe that the denoising results with the SDM's are better than the results with fixed sparsity degrees. The difference is more visible between the pre-filtering with a sparsity equals to three and the denoised result with the corresponding SDM. The pre-filtering with a sparsity degree equals to one presents a lower PSNR than the result with the corresponding SDM but they seem very similar. We explain this by the fact that most of the patches are homogenenous, hence, represented with a sparsity degree equals to one in the SDM. Note that the denoising result using the SDM with a sparsity degree equals to one is better than the one using the SDM with a sparsity degree equals to three. Consequently, we will use in the sequel a sparsity degree equals to one to pre-filter the images with the positive side effect that it decreases computation time.

Note that, since the denoising framework is very simple, it is normal that the results are not competitive with the state of the art. The aim of this study is to prove that the visual quality and the PSNR obtained while using the sparsity maps are better than the ones obtained with a fixed sparsity degree for all the patches. Hence, with such a simple denoising framework, we expect that there will still be an improvement with a more sophisticated denoising framework and a better dictionary in the SAR image case, as investigated in section V. We also would like to stress that, indeed, it is possible not to use the same sparsity degree for all the patches during the sparse-coding and use a low error rate as stopping criterion instead. It works very well in the Gaussian case (see fig. 2), however, this is not th case with speckle noise and it increases the computation time. This point will be further discussed in section V-B.

SA with low error rate, 28.39 dB

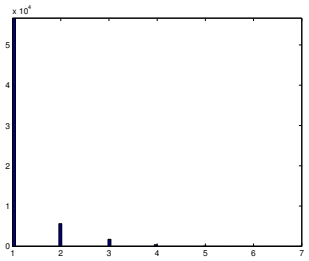

Proportion of patches as a function of sparsity degree

Fig. 2. On the left: Barbara image denoised by SA (Sparse Approximation) of each patch with an OMP. The sparsity degree is not fixed for all the patches, the stopping criterion is a low error-rate. On the right: histogram of the sparsity degrees used to represent the patches in Barbara. We observe that the most used sparsity degrees range from 1 to 3.

IV. Proposed sparse-coding procedure dedicated to SAR images

In order to process properly SAR images, the despeckling methods used should be adapted to the statistics of speckle noise. In this section, we propose a sparse-coding procedure adapted to logarithmically-transformed SAR data. Hence we use a Fisher-Tippett distribution as data-fidelity term which corresponds to the logarithm of the gamma distribution often used to model intensity SAR images. The whole sparse-coding problem is expressed by the next equation:

$$\{\hat{\boldsymbol{x}}, \hat{\boldsymbol{u}}\} = \underset{\boldsymbol{u},\boldsymbol{x}}{\operatorname{argmin}} \sum_{i=1}^{N} \lambda(x_i - y_i + \exp(y_i - x_i)) + \mu||\boldsymbol{u}_i||_0 \quad (5)$$

where $\boldsymbol{x}$ is the image to recover, $\hat{\boldsymbol{x}}_i = \boldsymbol{D}\hat{\boldsymbol{u}}_i$ the i-th patch from the restaured image $\hat{\boldsymbol{x}}$, $\boldsymbol{y}$ the speckled image, x_i, y_i are pixels extracted from $\boldsymbol{x}, \boldsymbol{y}$ respectively at position i and N the number of pixels.

This optimization problem is difficult to solve. A possible strategy is to use ans iterative appraoch called half-quadratic splitting, as it is proposed for instance in [21]. It implies to introduce for each patch an auxiliary variable $\boldsymbol{z}_i = \boldsymbol{D}\boldsymbol{u}_i$ which will allow us to optimize the fonction alternatively along $\boldsymbol{x}$ and $\boldsymbol{z}_i$:

$$\{\hat{\boldsymbol{x}}, \hat{\boldsymbol{u}}\} = \underset{\boldsymbol{u},\boldsymbol{x}}{\operatorname{argmin}} \sum_{i=1}^{N} \lambda(x_i - y_i + \exp(y_i - x_i)) \quad (6)$$
$$+ \min_{\boldsymbol{z}_i} \frac{\delta}{2}||\boldsymbol{R}_i\boldsymbol{x} - \boldsymbol{z}_i||^2 + \mu||\boldsymbol{u}_i||_0$$

where $\boldsymbol{R}_i$ is the extracting operator of the i-th patch in the image.

Note that the square difference between $\boldsymbol{R}_i\boldsymbol{x}$ and $\boldsymbol{z}_i$ can be rewritten this way:

$$\sum_i \|\boldsymbol{R}_i\boldsymbol{x} - \boldsymbol{z}_i\|^2 = \sum_i c_i(x_i - \bar{z}_i)^2 \quad (7)$$

where $\bar{\boldsymbol{z}} = \operatorname{diag}(\boldsymbol{c})^{-1} \sum_i \boldsymbol{R}_i^t \boldsymbol{z}_i$ is the uniform reprojection of the patches $\boldsymbol{z}_i$ in the image domain, and c_i is the number of patches $\boldsymbol{R}_i\boldsymbol{x}$ projecting on the pixel i. Hence, solving problem (6) along $\boldsymbol{z}_i$ can be performed by an OMP and solving it along $\boldsymbol{x}$ boils down to solving the next problem:

$$\{\hat{\boldsymbol{x}}\} = \underset{\boldsymbol{x}}{\operatorname{argmin}} \sum_{i=1}^{N} \left[\lambda(e^{y_i - x_i} + x_i - y_i) + \frac{\delta}{2} c_i (x_i - \bar{z}_i)^2\right] \quad (8)$$

which can be solved with a few iterations of the Newton method (10 are enough) as described by the next equation at iteration $t+1$:

$$x_i^{(t+1)} = x_i^{(t)} - \frac{\lambda(1 - e^{y_i - x_i^{(t)}}) + \delta c_i (x_i^{(t)} - \bar{z}_i))}{\lambda e^{y_i - x_i^{(t)}} + \delta c_i} \quad (9)$$

In theory, as $\delta \to \infty$ the algorithm converges. In practice, a few iterations (three or four) are enough to obtain a good solution. Algorithm 1 describes the whole SAR-sparse-coding (SAR-SC) procedure proposed. The values of δ are incresing from one iteration to another as mentioned in [22] and in its adaptation to SAR data [23] that also use half-quadratic splitting (with a GMM prior).

Algorithm 1 SAR-SC

Require: N_{pa} : number of patches, N_{pi} : number of pixels, N_{it} : number of iterations,
Initialization: $\boldsymbol{x}_i = \boldsymbol{y}_i, \forall i \in \{1, ..., N_{\text{pa}}\}$
for $\delta = [1, 4, 8, 16]/\psi(1, L)$ **do**
  for $i \in \{1, ..., N_{\text{pa}}\}$ **do**
    Use an OMP to obtain $\hat{\boldsymbol{u}}_i$
    Update $\boldsymbol{z}_i = \boldsymbol{D}\hat{\boldsymbol{u}}_i$
  end for
  for $t = 0$ to $N_{\text{it}} - 1$ **do**
    for $p \in \{1, ..., N_{\text{pi}}\}$ **do**
      Update $x_p^{(t+1)}$ with eq. (9)
    end for
  end for
end for

V. Results on SAR images and discussion

A. Implementation details of the despeckling procedure

1) About the dictionary: The dictionary used in the proposed approach is learned offline with the K-SVD algortihm applied on logarithmically transformed multi-look SAR data (see the data-base in fig. 4). The parameters of the algorithm are the same as in the original paper except that the noise level is adapted to SAR data and the number of looks. Consequently, we didn't set a fixed sparsity degree in the OMP and the stopping-criterion was a low error rate. The initialization is a DCT (Discrete Cosine Transform) dictionary. The dictionary obtained is presented in figure 5. It is satisfying because the algorithm managed to capture targets which are important features in SAR data and edges with various orientations.

2) Main steps of the proposed algorithm: The next steps summarize the proposed despeckling algorithm:

- An initial despeckling result is computed in order to obtain the CVM. To this end, the despeckling procedure

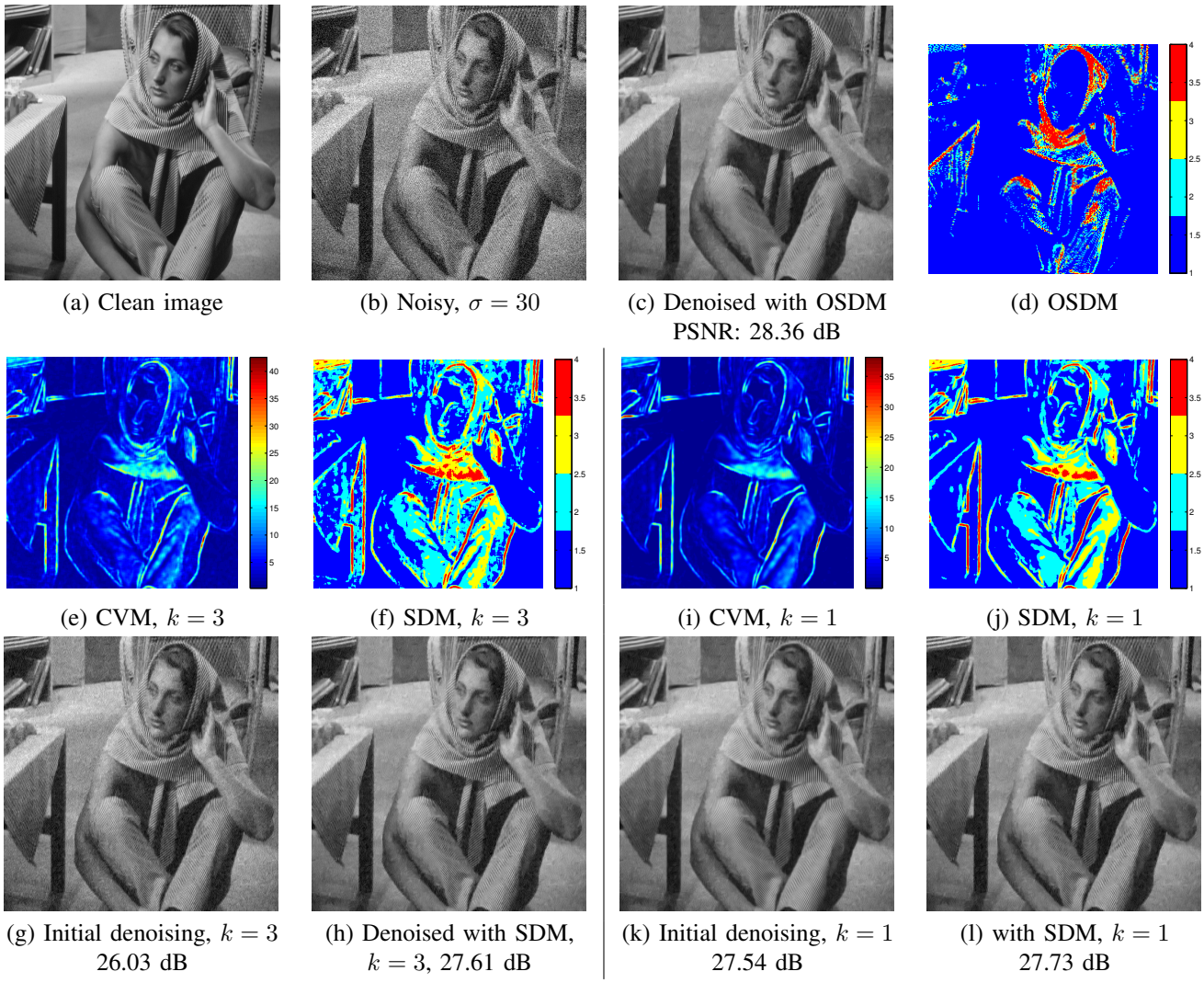

(a) Clean image (b) Noisy, $\sigma = 30$ (c) Denoised with OSDM PSNR: 28.36 dB (d) OSDM

(e) CVM, $k = 3$ (f) SDM, $k = 3$ (i) CVM, $k = 1$ (j) SDM, $k = 1$

(g) Initial denoising, $k = 3$ 26.03 dB (h) Denoised with SDM, $k = 3$, 27.61 dB (k) Initial denoising, $k = 1$ 27.54 dB (l) with SDM, $k = 1$ 27.73 dB

Fig. 3. In this figure, the appearance of the Oracle-SDM and the SDM's obtained with two different sparsity degrees are compared. The performance of the proposed approach based on the hypothesis that we should use a map to indicate the best sparsity degree for each patch to improve the denoising results of a sparsity-based approach is also evaluated. As expected, the result with the OSDM provides best PSNR and the proposed approach with the SDM's gives a better result than with a fixed sparsity for all the patches in the image.

described in section IV is applied with a sparsity degree $k = 1$.

- The CVM is obtained the same way as described in section III-B except that the coefficient of variation is computed on locarithmically transformed patches.
- The SDM is computed the same way as described in section III-B.
- The SDM and the proposed sparse-coding procedure are used to despeckle each patch with the prescribed sparsity degree in the map.

Figure 6 shows preliminary results on real SAR images. We observe that the SDM's are satisfying. We also observe that backscaterring targets are better restaured in the proposed approach than with the initial despeckling result used to compute the CVM. In the next paragraph we explain how to enhance those results in homogeneous areas.

3) Improving despeckling results in homogeneous areas: As we can observe in the preliminary results in figure 6, there is an improvement between the visual quality of the initial denoising and the proposed method in complex structures. However, homogeneous areas need more smoothing. To tackle this issue, we propose to represent the patches with a sparsity degree equals to one (which are homogeneous) in the SDM with a specific small dictionary composed of 12 constant atoms (with values ranging from 20 to 160). Note that, in the sparse-coding algorithm, without improvement of homogeneous areas, we set $\delta = [1, 4, 8]/\psi(1, L)$ and with improvement: $\delta = [1, 4, 8, 16]/\psi(1, L)$ in order to obtain a better despeckling result. Some results with this improvement are presented in figure 9. We observe that edges and backscatterring targets are well preseved and homogeneous areas are smoother than in the result without improvement.

B. Comparisons with other methods

1) Comparison with low error rate sparse approximation: In this paper, we demonstrated in a denoising taske that it is better to use a SDM in comparison with using the same sparsity degree to approximate each patch extracted from an image. In the Gaussian noise case, it is better to use a sparse approximation with a low error rate stopping criterion in

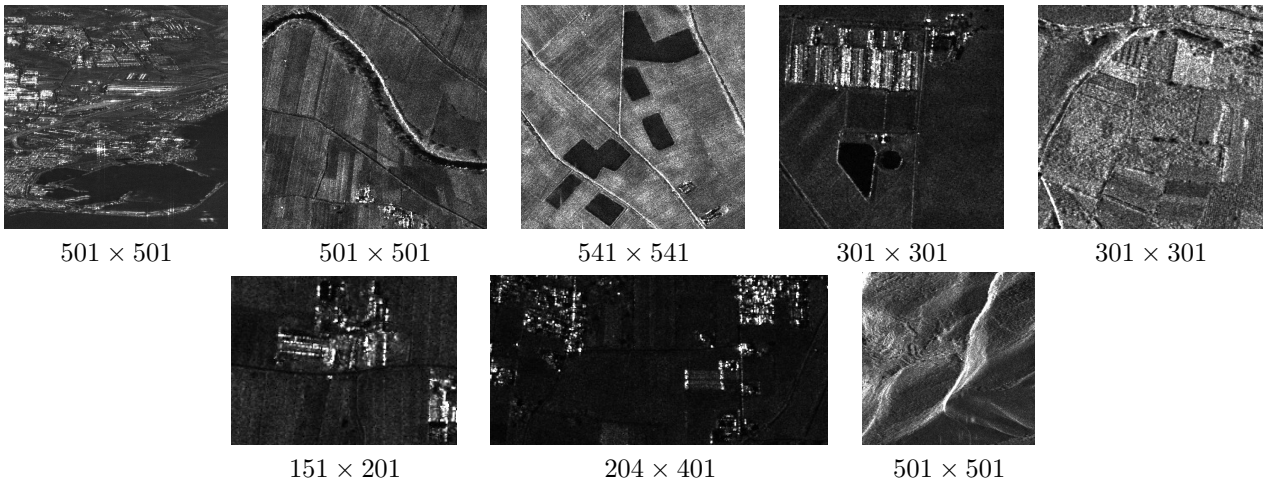

Fig. 4. Data-base composed of various SAR images used to learn the K-SVD dictionary.

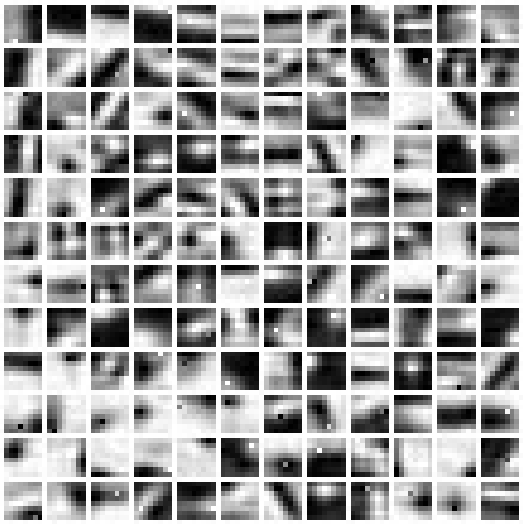

Fig. 5. K-SVD dictionary learned on logarithmically-transformed SAR data. It is composed of 144 atoms of size 8×8.

comparison with a sparse approximation with a SDM. In this paragraph, we investigate if this assertion remains true in the SAR image case. Figure 8 shows results on a real SAR image and a natural image with synthetic 2-looks speckle noise. It allows us to compare the sparse-coding approach adapated to SAR data with low-error-rate stopping criterion and with the SDM. We observe that with both real and synthetic noise, low-error-rate sparse approximation results are blurrier than the result obtained with the proposed approach especially with 4 iterations (with $\delta = [1, 4, 8, 16]/\sigma^2$). The PSNR values computed on the natural image confirm this observation. It also should be noted that, in the SAR image case, the computation time is shorter with the porposed approach. A possible justification is that, since the dynamic range of SAR images is high in comparison with natural images, the error is high too, hence the LER sparse-coding reaches the desired precision slowly.

2) Comparison with another type of map: In this paragraph, we estimate the optimal sparsity for each patch with a different method. This new map is computed using a criterion based on a GLR (Generalized Likelihood Ratio) test presented in [24] which boils down to an improvement of a ratio between the arithmetic mean and the geometric mean. Once this criterion is computed, the K-means algorithm is applied on the inital map as it is done with the SDM. In figure 9, results obtained using the SDM and the new map called Soft Classification Weight Map (SCWM) are compared. We observe that this map is as relevant as the SDM and it tends to associte more patches to the sparsity degree equals to 4 than the SDM. In spite of this difference, the despeckling results are quite similar except that less oversmoothing is observed with the SCWM.

3) Comparisons with state of the art and a sparsity-based methods: In this section, we compare the proposed method with methods using sparse representations and state of the art despeckling algorithms. Most of state of the art approaches are based on patch similarity such as SAR-BM3D [25] and PPB, Probabilistic Patch-Based filter [26] (which has been improved through NL-SAR algorithm [27]). These algorithms are adaptations of BM3D, Block-Matching 3D [28] and Non-Local means algorithm [29] to SAR data respectively. Concerning, a sparsity-based approach, H-K-SVD (Homomorphic K-SVD) uses an ℓ_0 prior. It is the original K-SVD algorithm [30] applied to the logarithm of the SAR image with a debiasing step [31]. We observe in figure 10 that our result:

- doesn't introduce artifacts in homogeneous areas as it can be observed with SAR-BM3D and FANS;
- doesn't present the artifact of isolated dark pixels as in H-K-SVD, which happens when the data-fidelity term isn't adapted to SAR data.
- is comparable with the PPB result but doesn't suffer from patch-rare effect.

VI. Conclusions

In this paper, we first proposed a new sparse-coding algorithm adapted to SAR images and the coresponding despeckling procedure. Then, we studied how does a map which estimates the optimal sparsity-degree for each patch improve the quality of the despeckling in comparison with two methods. The first one is the standard sparse-coding procedure with a low-error-rate stopping criterion. The second one is a sparse-coding procedure which imposes the same sparsity degree for each patch. In the low-error-rate approach, the sparsity degree is not fixed for each patch and the algorithm

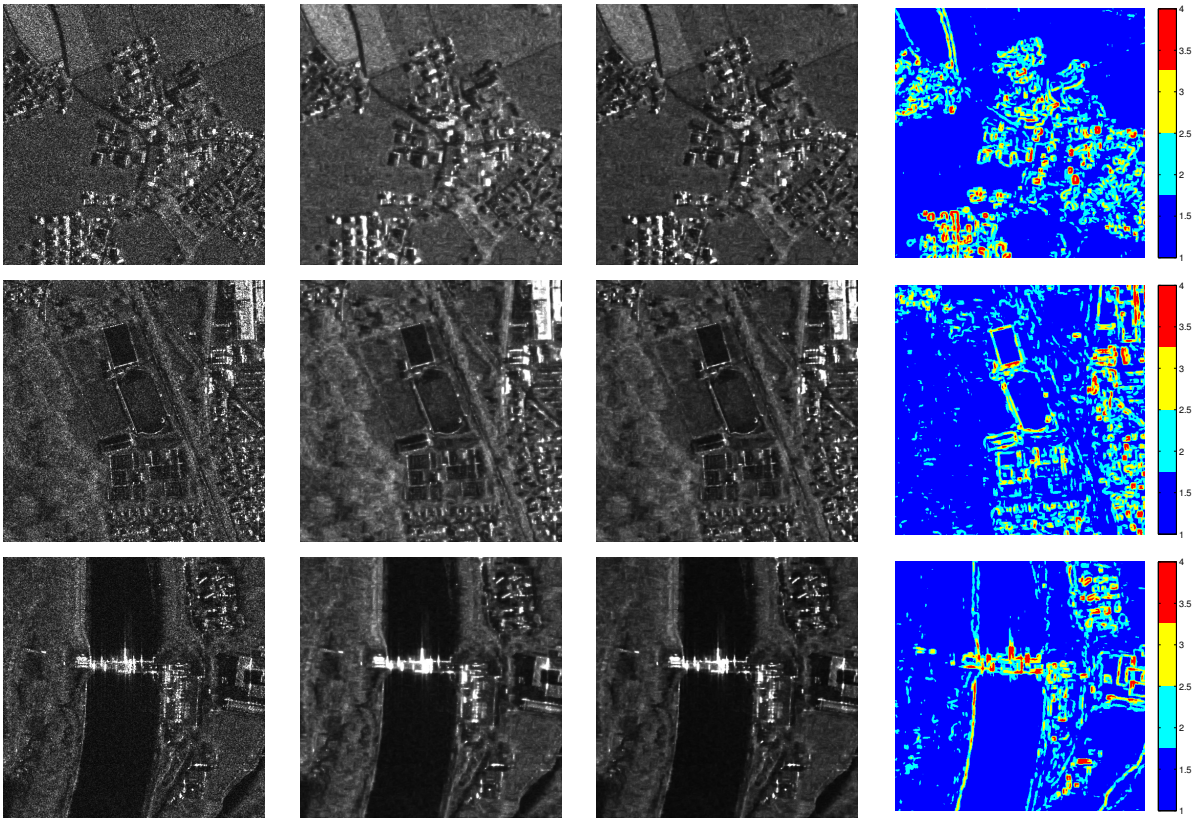

Fig. 6. Preliminary results. The initial despeckling is obtained with fixed sparsity degree equals to one et and the proposed approach uses for each patch te sparsity-degree estimated in the map, hence we notice improvements in the reconstruction of backscaterring targets for instance.

stops when the difference between the approximation of the patches at iteration (t) and at iteration $(t+1)$ is below a specified precision. The low-error-rate method provides the best results in the Gaussian noise case. However, in the SAR image case, the proposed approach gives better results than both procedures. In fact, speckle noise is so strong that the error is very high from one iteration to another and the low-error-rate approach becomes very slow and gives a blurry result. In the furutre, we will evaluate this difference of speed and compute measures described in [32] in order to obtain quatitative comparison of our results with state of the art.

REFERENCES

[1] M. Aharon, M. Elad, and A.M. Bruckstein, "The K-SVD: An algorithm for designing of overcomplete dictionaries for sparse representation," *IEEE Trans. on Signal Processing*, vol. 54, no. 11, pp. 4311–4322, 2006.

[2] Scott Shaobing Chen, David L Donoho, and Michael A Saunders, "Atomic decomposition by basis pursuit," *SIAM Journal on Scientific Computing*, vol. 20, no. 1, pp. 33–61, 1998.

[3] Y.C. Pati, R. Rezaiifar, and P.S. Krishnaprasad, "Orthogonal matching pursuit: recursive function approximation with applications to wavelet decomposition," in *Proceedings of 27th Asilomar Conference on Signals, Systems and Computers*, Nov 1993, pp. 40–44 vol.1.

[4] Jiang Jiang, Liangwei Jiang, and Nong Sang, "Non-local sparse models for SAR image despeckling," in *Computer Vision in Remote Sensing (CVRS), 2012 International Conference on*. IEEE, 2012, pp. 230–236.

[5] Caner Ozcan, Baha Sen, and Fatih Nar, "Sparsity-driven despeckling for SAR images," *IEEE Geoscience and Remote Sensing Letters*, vol. 13, no. 1, pp. 115–119, 2016.

[6] Maryam Amirmazlaghani and Hamidreza Amindavar, "A novel sparse method for despeckling SAR images," *IEEE Transactions on Geoscience and Remote Sensing*, vol. 50, no. 12, pp. 5024–5032, 2012.

[7] Julien Mairal, Francis Bach, Jean Ponce, and Guillermo Sapiro, "Online dictionary learning for sparse coding," in *International conference on machine learning*. ACM, 2009, pp. 689–696.

[8] T. Lu, S. Li, L. Fang, and J-A. Benediktsson, "SAR image despeckling via structural sparse representation," *Sensing and Imaging*, vol. 17, no. 1, pp. 1–20, 2016.

[9] Bin Xu, Yi Cui, Zenghui Li, and Jian Yang, "An iterative SAR image filtering method using nonlocal sparse model," *IEEE Geoscience and Remote Sensing Letters*, vol. 12, no. 8, pp. 1635–1639, 2015.

[10] Joel A Tropp, Anna C Gilbert, and Martin J Strauss, "Algorithms for simultaneous sparse approximation. part i: Greedy pursuit," *Signal Processing*, vol. 86, no. 3, pp. 572–588, 2006.

[11] Julien Mairal, Francis Bach, Jean Ponce, Guillermo Sapiro, and Andrew Zisserman, "Non-local sparse models for image restoration," in *IEEE 12th International Conference on Computer Vision*, 2009, pp. 2272–2279.

[12] Bradley Efron, Trevor Hastie, Iain Johnstone, Robert Tibshirani, et al., "Least angle regression," *The Annals of statistics*, vol. 32, no. 2, pp. 407–499, 2004.

[13] Yu Han, Xiang-Chu Feng, George Baciu, and Wei-Wei Wang, "Non-convex sparse regularizer based speckle noise removal," *Pattern Recognition*, vol. 46, no. 3, pp. 989–1001, 2013.

[14] J.M. Bioucas-Dias and M. A. Figueiredo, "Multiplicative noise removal using variable splitting and constrained optimization," *IEEE Transactions on Image Processing*, 2010.

[15] Weisheng Dong, Guangming Shi, and Xin Li, "Nonlocal image restoration with bilateral variance estimation: a low-rank approach," *IEEE transactions on image processing*, vol. 22, no. 2, pp. 700–711, 2013.

[16] Chenglong Wang, Guanghui Zhao, Guangming Shi, and Huan Li, "SAR image despeckling based on the nonlocally centralized sparse representation model," in *International Conference on Computer and Information Technology (CIT)*. IEEE, 2014, pp. 143–147.

[17] Weisheng Dong, Lei Zhang, and Guangming Shi, "Centralized sparse representation for image restoration," in *International Conference on Computer Vision*. IEEE, 2011, pp. 1259–1266.

[18] S. Foucher, "SAR image filtering via learned dictionaries and sparse

representations," in *IEEE International Geoscience and Remote Sensing Symposium, IGARSS*. IEEE, 2008, vol. 1, pp. I–229.

[19] Fatih Porikli, Rajagopalan Sundaresan, and Kei Suwa, "Sar despeckling by sparse reconstruction on affinity nets (SRAN)," in *European Conference on Synthetic Aperture Radar, EUSAR*. VDE, 2012, pp. 796–799.

[20] P. Chainais, "Towards dictionary learning from images with non gaussian noise," in *IEEE International Workshop on Machine Learning for Signal Processing (MLSP)*. IEEE, 2012, pp. 1–6.

[21] J. Sulam and M. Elad, "Expected patch log likelihood with a sparse prior," in *International Workshop on Energy Minimization Methods in Computer Vision and Pattern Recognition*. Springer, 2015, pp. 99–111.

[22] D. Zoran and Y. Weiss, "From learning models of natural image patches to whole image restoration," in *IEEE International Conference on Computer Vision (ICCV)*, Nov 2011, pp. 479–486.

[23] S. Tabti, C-A. Deledalle, L. Denis, and F. Tupin, "Modeling the distribution of patches with shift-invariance: Application to SAR image restoration," in *IEEE International Conference on Image Processing (ICIP)*, Oct 2014, pp. 96–100.

[24] Diego Gragnaniello, Giovanni Poggi, Giuseppe Scarpa, and Luisa Verdoliva, "SAR despeckling based on soft classification," in *IEEE International Geoscience and Remote Sensing Symposium (IGARSS)*. IEEE, 2015, pp. 2378–2381.

[25] S. Parrilli, M. Poderico, C.V. Angelino, and L. Verdoliva, "A non-local SAR image denoising algorithm based on LLMMSE wavelet shrinkage," *IEEE Transactions on Geoscience and Remote Sensing*, vol. 50, no. 2, pp. 606–616, 2012.

[26] C-A. Deledalle, L. Denis, and F. Tupin, "Iterative weighted maximum likelihood denoising with probabilistic patch-based weights," *IEEE Transactions on Image Processing*, vol. 18, no. 12, pp. 2661–2672, 2009.

[27] C-A. Deledalle, L. Denis, F. Tupin, A. Reigber, and M. Jäger, "NL-SAR: A unified non-local framework for resolution-preserving (Pol)(In) SAR denoising," *IEEE Transactions on Geoscience and Remote Sensing*, vol. 53, no. 4, pp. 2021–2038, 2015.

[28] Kostadin Dabov, Alessandro Foi, Vladimir Katkovnik, and Karen Egiazarian, "Image denoising by sparse 3-D transform-domain collaborative filtering," *IEEE Transactions on Image Processing*, vol. 16, no. 8, pp. 2080–2095, 2007.

[29] A. Buades, B. Coll, and J.-M. Morel, "A non-local algorithm for image denoising," in *IEEE Computer Society Conference on Computer Vision and Pattern Recognition, CVPR*, June 2005, vol. 2, pp. 60–65 vol. 2.

[30] M. Elad and M. Aharon, "Image denoising via sparse and redundant representations over learned dictionaries," *IEEE Transactions on Image Processing*, vol. 15, no. 12, pp. 3736–3745, 2006.

[31] H. Xie, L.E. Pierce, and F.T. Ulaby, "SAR speckle reduction using wavelet denoising and Markov random field modeling," *IEEE Transactions on Geoscience and Remote Sensing*, vol. 40, no. 10, pp. 2196–2212, Oct 2002.

[32] Gerardo Di Martino, Mariana Poderico, Giovanni Poggi, Daniele Riccio, and Luisa Verdoliva, "Benchmarking framework for SAR despeckling," *IEEE Transactions on Geoscience and Remote Sensing*, vol. 52, no. 3, pp. 1596–1615, 2014.

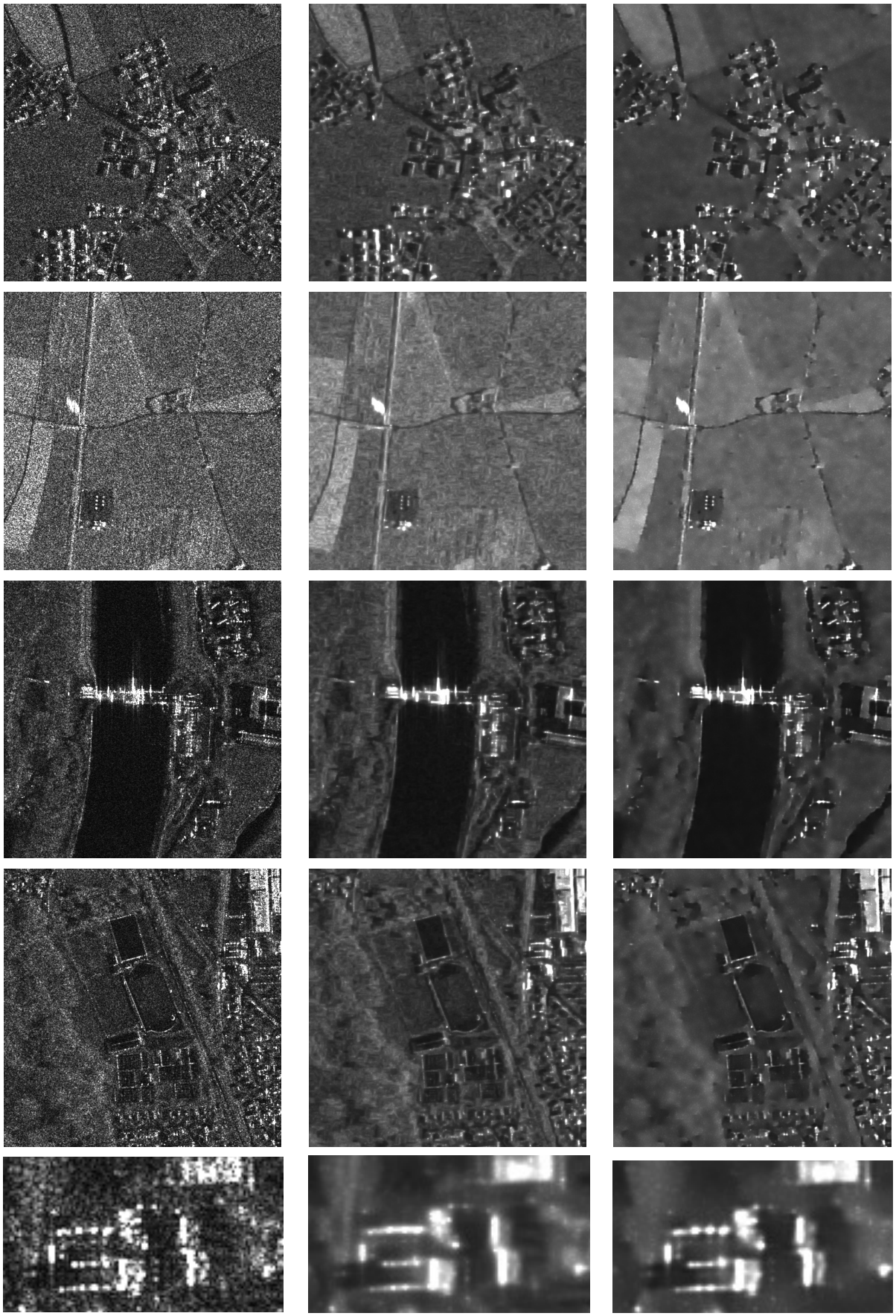

SAR image | Initial despeckling, $k = 1$ | Improved result

Fig. 7. Some results with the homogeneous areas improvement using a set of constant patches where the estimated sparsity-degree in the SDM is equal to one. The last row is a zoom of the results on the row before the last.

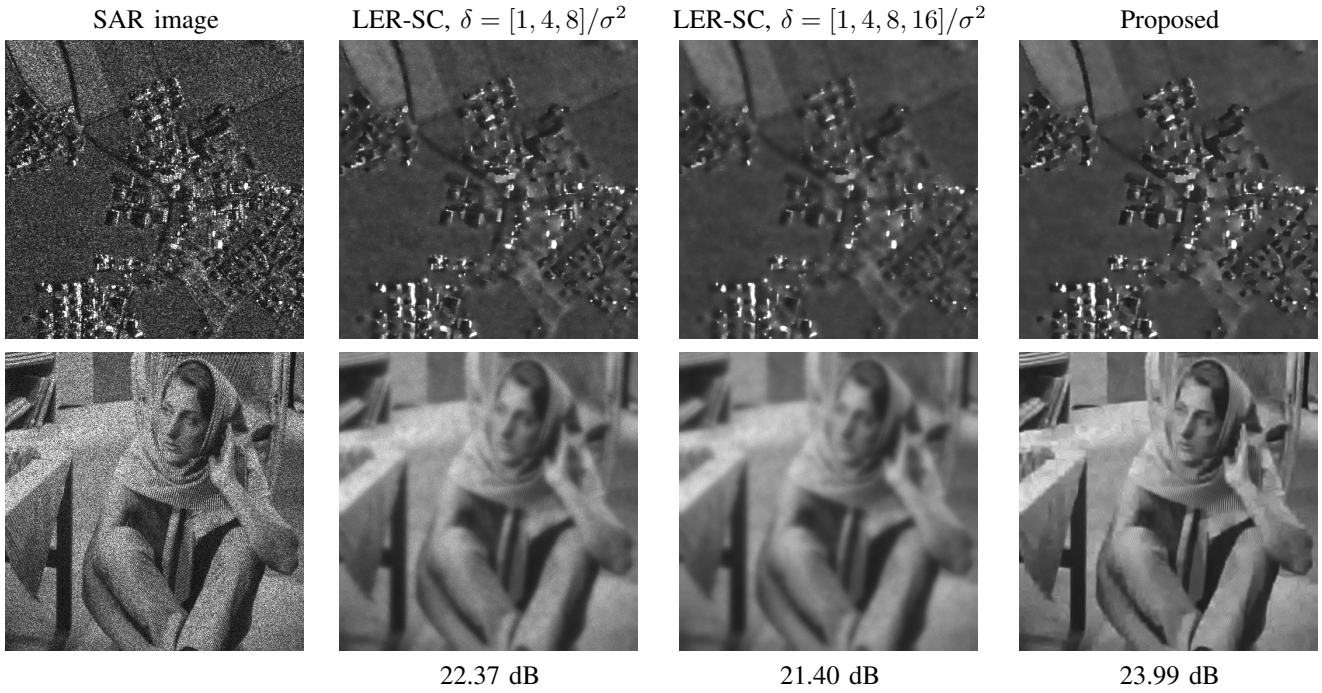

Fig. 8. Notations: SC= Sparse Coding, LER= Low Error Rate. We observe with both synthetic and real speckle noise that the result of the proposed method is less blurry than the LER results espcially with $\delta = [1, 4, 8, 16]/\sigma^2$. In the SAR image case, if we zoom in, we can observe a stronger "white dots effect" in homogeneous areas of the LER results, in particular with $\delta = [1, 4, 8]/\sigma^2$. In addition to this we recall that our approach is faster than the LER-SC.

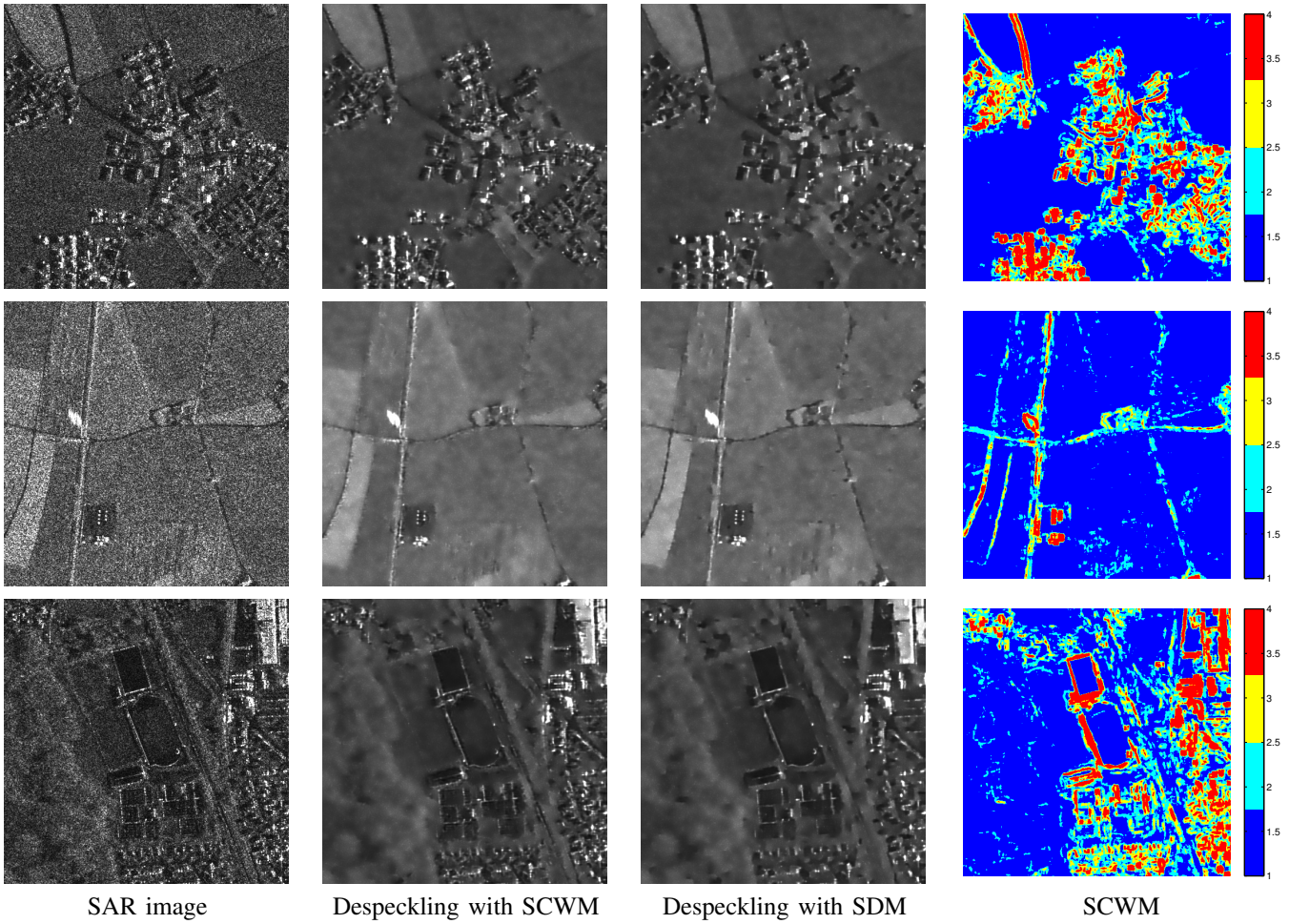

Fig. 9. Comparison between proposed approach using Soft Classification Weight Map (SCWM) and the SDM based on the coefficient of variation. We observe that details in urban areas are better preserved with SCWM and there is less oversmoothing except for the image in the second row.

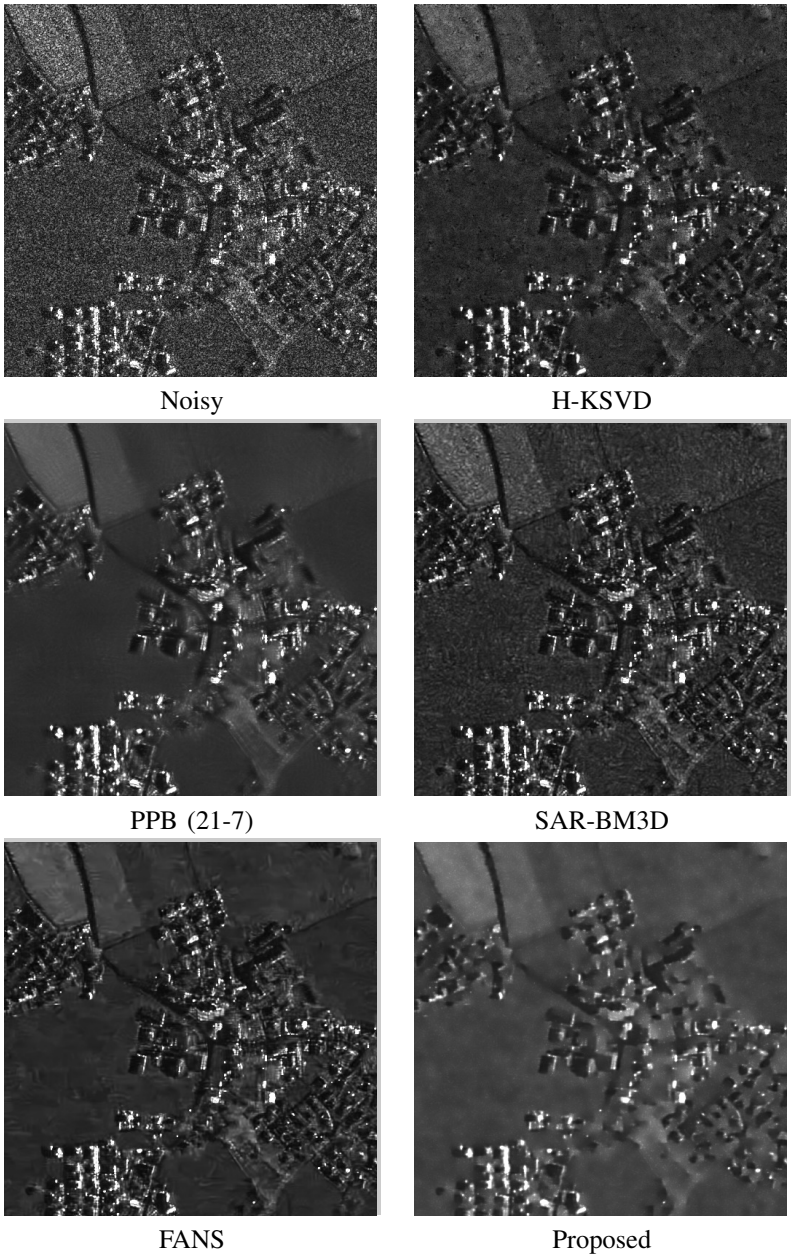

Fig. 10. Comparison of the proposed method with state of the art patch-based approaches.